

Ionic polymer-metal composite as energy harvesters

Rashi Tiwari, Kwang J. Kim* and Sang-Mun Kim

Department of Mechanical Engineering, University of Nevada, Reno, NV 89557, USA

(Received May 1, 2007, Accepted March 3, 2008)

Abstract. The ability of an electroactive polymer, IPMC (Ionic Polymer Metal Composites,) to produce electric charge under mechanical deformations may be exploited for the development of next generation of energy harvesters. Two different electrode types (gold and platinum) were employed for the experiments. The sample was tested under dynamic conditions, produced through programmed shaking. In order to evaluate the potential of IPMC for dry condition, these samples were treated with ionic liquid. Three modes of mechanical deformations (bending, tension and shear) were analyzed. Experimental results clearly indicate that IPMCs are attractive applicants for energy harvesting, with inherent advantages like flexibility, low cost, negligible maintenance and virtually infinite longevity. Besides, preliminary energy harvesting model of IPMC has been formulated based upon the work of previous investigators (Newbury 2002, Newbury and Leo 2002, Lee, *et al.* 2005, Konyo, *et al.* 2004) and the simulation results reciprocate experimental results within acceptable error.

Keywords: ionic polymer metal composites; energy harvesting; sensor model.

1. Introduction

Electroactive Polymer (EAP) is the material that could produce charge on mechanical deformation or undergo a mechanical deformation under the influence of an electric field. EAPs are generally classified as electronic or ionic materials. Ionic Polymer Metal Composite (IPMC) which is the base material for the development of sensor in this paper falls under the category of ionic type EAP. Table 1 compared the properties of IPMC with PZT (Lead Zirconate Titanate).

The underlying sensing and actuation mechanism of IPMC, in a bending configuration, have been illustrated in Fig. 1 in a simplified manner. Applied mechanical bending causes cation density to increase on compressed side, and to decrease on the stretched side (Kothera, 2002). In order to restore ion balance inside the polymeric membrane, cations migrate from higher to lower density region, producing charge. Similarly, on application of electric field across the IPMC, cations migrate towards the negative polarity region of the field. Consequently, cation repulsion supplemented by high density cause the membrane to bend.

IPMC as sensor may be employed for the purpose of harvesting wasted mechanical energy, in the form of vibration. Numerous source of mechanical vibration may be taken into consideration like automobiles, health monitoring systems, ships, process instrumentations and aircrafts. The captured mechanical energy can be converted into useful electrical energy and stored for future use. An extensive review of the energy harvesting from vibration using piezoelectric materials has been presented in literature (Sodano, *et al.*

*Active Materials and Processing Laboratory, Corresponding Author, E-mail: kwangkim@unr.edu

Table 1 Comparison of properties between IPMC and PZT

Properties	Excitation voltage (V)	Displacement	Force generated	Power generation
IPMC	1-3	mm	mN	μ W
PZT	50-300	μ m	N	μ W

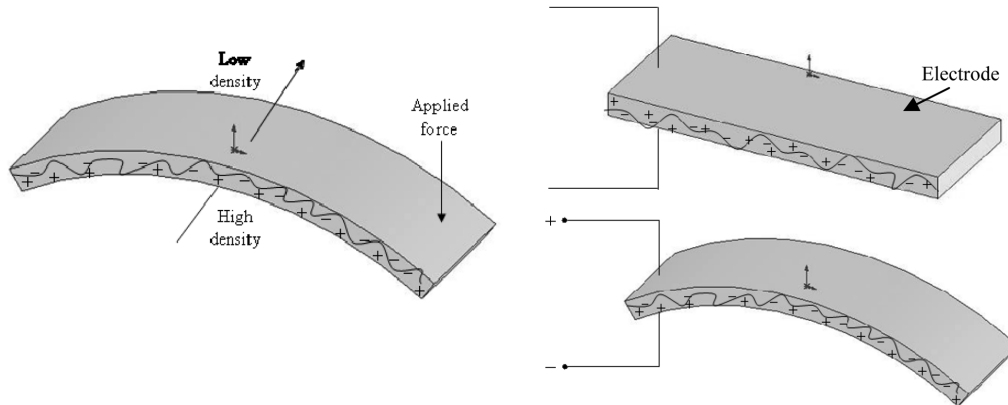


Fig. 1 IPMC sensor (left) and actuator (right) mechanism

Table 2 Different types of energy harvesters (Paradiso and Starner 2005)

Energy Source	Power	Advantages	Disadvantages
Ambient radio frequency	$< 1 \mu\text{W}/\text{cm}^2$		Have to be placed near transmitters
Ambient light	100 mW/cm ² (direct sunlight) 100 μ W/cm ² (indoor)	Good conversion efficiency	Power output vary greatly with the light source
Thermoelectric	60 μ W/cm ²	Small size	Low conversion efficiency
Vibration micro-generator	4 μ W/cm ³ (human motion in Hz) 800 μ W/cm ³ (KHz source)	Large structures can achieve higher power density	Highly dependent on excitation density

2004). Table 2 compares various energy harvesting methods like solar, temperature gradient and vibration. IPMC based energy harvesters fall into vibration based micro-generators.

This paper presents a proof of the proposed concept of using IPMC for energy harvesting applications. Besides, IPMC sensor model is being formulated for better understanding of the sensing and energy harvesting mechanism.

2. Electro-mechanical modeling

IPMC can be used as a mechano-electric sensor by clamping it between two electrodes shown in Fig. 1. Electro-mechanical modeling helps in better understanding of the system and its response. This type of modeling is usually represented by the transformer circuit (Newbury and Leo 2002) such as one shown in Fig. 2. For the purpose of simplicity it is assumed that the electrical and the mechanical component of the system are coupled linearly.

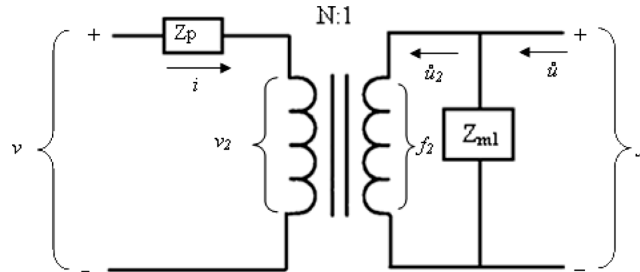


Fig. 2 Transformer circuit to represent the electro-mechanical model of IPMC

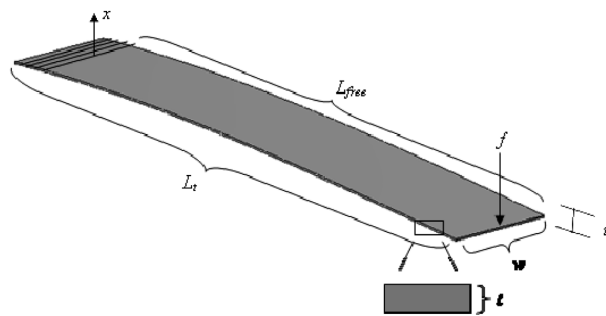


Fig. 3 Mechanical specification of IPMC

Applied mechanical force to the IPMC is represented by f and \dot{u} is the velocity of application of force. The electrical domain consists of electrical voltage, v , and current, i , produced by IPMC. The mechanical specification of the IPMC sample is provided in Fig. 3. The following derivation is simplification of modeling equations originally derived by Newbury (2002).

2.1. Mechanical components

Mechanical moment M , produced due to IPMC bending, as a function of the applied tip force, f .

$$M = f(L_d - x) \tag{1}$$

$$L_d = L_{free} \tag{2}$$

where, x is the distance from the supported end. Bending moment can be related to small deflections:

$$\frac{d^2 u}{dx^2} = \frac{M}{YI} \tag{3}$$

where, Y is the Young's modulus and I is the moment of inertia for the IPMC cantilever beam. Thus deflection of the IPMC beam is:

$$u(x) = \frac{f}{YI} \left[\frac{L_{free} x^2}{2} - \frac{x^3}{6} + C_1 x + C_2 \right] \tag{4}$$

The value of $C_1=C_2=0$ was determined at the boundary condition: $(x = 0, \dot{u}(x) = 0)$ and $(x = 0, u(x) =$

0), respectively. Therefore, Eq. (4) reduced to:

$$u(x) = \frac{f}{YI} \left[\frac{L_{free} x^2}{2} - \frac{x^3}{6} \right] \quad (5)$$

Moment of inertia for a rectangular beam is given by:

$$I = \frac{wt^3}{12} \quad (6)$$

Substituting Eq. (6) in Eq. (5), and evaluating displacement at $x = L_{free}$

$$u = f \frac{AL_{free}^3}{Ywt^3} \quad (7)$$

Also Z_{m_1} in the Laplace domain, in the circuit is given by

$$Z_{m_1} = \frac{f}{su} \quad (8)$$

Thus comparing Eq. (7) with Eq. (8), stiffness of the IPMC sample is calculated as:

$$Z_{m_1} = \frac{1}{s} \frac{Ywt^3}{4L_{free}^3} \quad (9)$$

2.2. Electrical components

It has been shown that IPMC displays resistive behavior at low (0-10Hz) and high frequencies (>100 Hz) (Konyo, *et al.* 2004). At intermediate frequencies (10-100Hz) it behaves like a capacitor. Since IPMC inherits both capacitive and resistive properties, it was modeled as a RC circuits (Kim, *et al.* 2006) as shown in Fig. 4 where R_i and C_i represent the two electrodes resistance and capacitance while R_e is the intrinsic resistance of NafionTM which is the base polymer material.

By following the previous work (Konyo, *et al.* 2004); we assume the properties of both electrodes are same. The Laplace transformation of impedance (Z) describing a RC circuit, shown in Fig. 4, with a step input is given by Eq. (10). Step input is used for the purpose of simplicity. Besides, DC voltage is conveniently used for IPMC actuation.

$$Z_p = 1 / \sum_{i=1}^n \frac{2R_i}{R_i C_i s + 1} + R_e \quad (10)$$

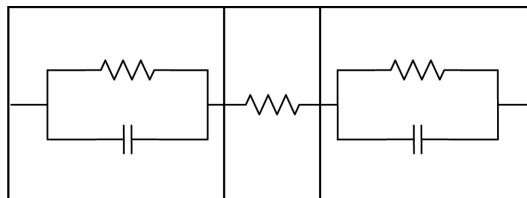


Fig. 4 Equivalent RC circuit model

$$R_i = \frac{\rho_i t}{L_i w}$$

$$C_i = \frac{\varepsilon_i L_i w}{t} \quad (11)$$

In the above equations, ρ_i is resistivity, and ε_i is permittivity of IPMC sample.

2.3. Electro-mechanical coupling:

The transformer circuit previously shown in Fig. 2 has a turn ratio N which represents the electro-mechanical coupling. This turn ratio presents the relationship between open-circuit voltage and the external force acting on the polymer:

$$\frac{v}{N} = \frac{f}{1} \quad \text{with } i = 0 \quad (12)$$

The constitutive equation of IPMC based upon small deflections may be derived based on the constitutive equation of piezoelectricity.

$$S = s^E T + dE$$

$$D = dT + \varepsilon^T E \quad (13)$$

where S and D represent strain and charge density, T and E are the applied stress and the electric field respectively. Variables s^E and ε^E are the short-circuit compliance and permittivity at zero applied stress, respectively.

The coefficient d in case of IPMC can be given by (Lee, *et al.* 2005)

$$d = \frac{2ut}{3L_{free}^2 \nu} \quad (14)$$

The surface stress T of IPMC can be related to the force by:

$$T = \frac{Nt}{2I} \quad (15)$$

Substituting Eq. (2) in Eq. (15)

$$T(x) = \frac{f(L_{free} - x)t}{2I} \quad (16)$$

Both sides of Eq. (13) are integrated over the IPMC sample width w and length L_t to transform the charge density to the total charge.

$$Q = \frac{3dL_{free}^2 f}{t^2} + \frac{\varepsilon^T L_t w}{t} \nu \quad (17)$$

In order to calculate the value of N , set $Q = 0$ in Eq. (17) and solve for ν/f .

$$N = \frac{3dL_{free}^2}{\varepsilon^T L_f \omega t} \quad (18)$$

Various input-output relations can also be obtained from the transformer circuit in Fig. 2. Mesh equations are calculated for analyzing the relationship between voltage and current for an ideal transformer.

$$Z_p i + v_2 = v$$

$$f_2 = f$$

$$f = Zm_1(\dot{u} - \dot{u}_2)$$

$$\frac{v_2}{N} = \frac{f_2}{1}$$

$$-iN = \dot{u}_2 \quad (19)$$

Hence we get,

$$\begin{Bmatrix} v \\ f \end{Bmatrix} = \begin{bmatrix} (Z_p + Zm_1 N^2) & Zm_1 N \\ Zm_1 N & Zm_1 \end{bmatrix} \begin{Bmatrix} i \\ \dot{u} \end{Bmatrix} \quad (20)$$

3. Experimental procedure

Tests are conducted to capture IPMC voltage produced under deformation conditions: bending, extension and shear as shown in Fig. 5. In case of bending and extension one end of the IPMC is constrained and both ends are constrained for shear mode. Fig. 6 shows the corresponding output signals produced by IMPC test samples (ionic liquid treated Platinum-IPMC of size 63 mm × 8.6 mm × 0.2 mm). A test shaker is used for inducing mechanical deformation for bending mode with a frequency of 10Hz sine wave signal. While extension and shear modes are performed at 1 and 0.1 Hz, respectively. “Polarity” (shown in Fig. 6(b) & (c)) refers to the electrode placement direction.

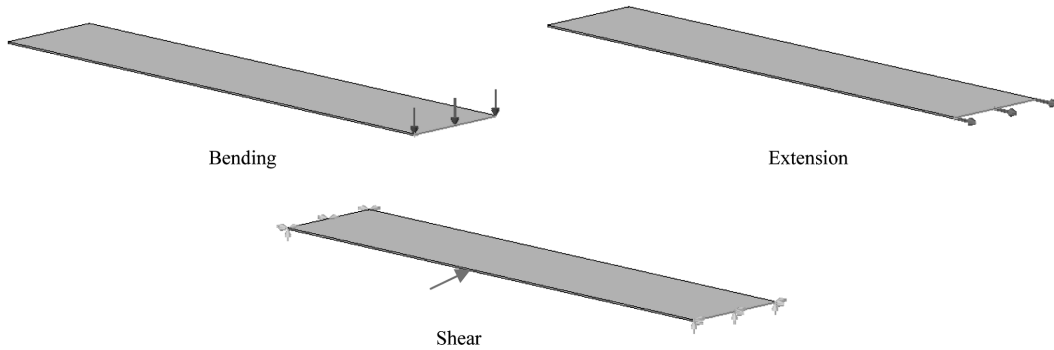


Fig. 5 Deformation modes of IPMC for energy harvesting experiment

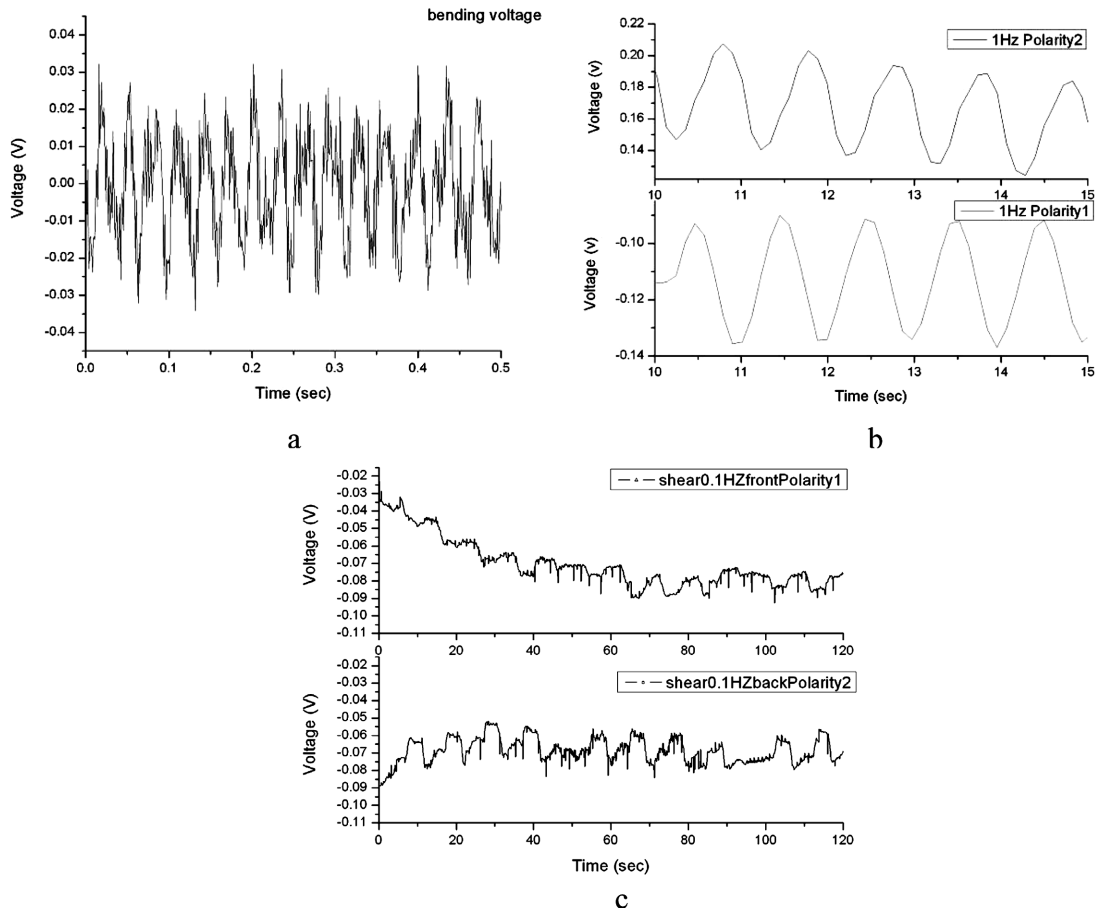


Fig. 6 Sensor voltage output from (a) bending, (b) tension and (c) shear mode

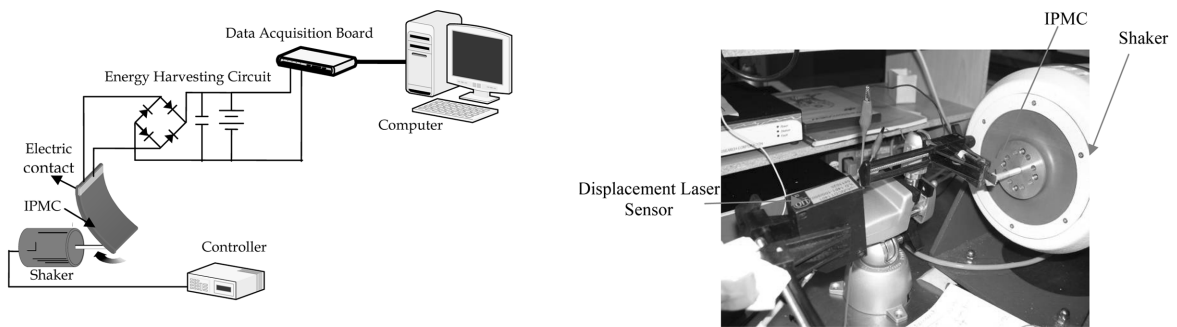


Fig. 7 Schematic of energy harvesting experimental set-up using shaker in bending mode

3.1. Bending mode

Schematic of experimental set-up for energy harvesting is shown in Fig. 7. A shaker assembly (TIRA Vibration System, TV52110) is used as the source of mechanical input. The shaker is programmed to

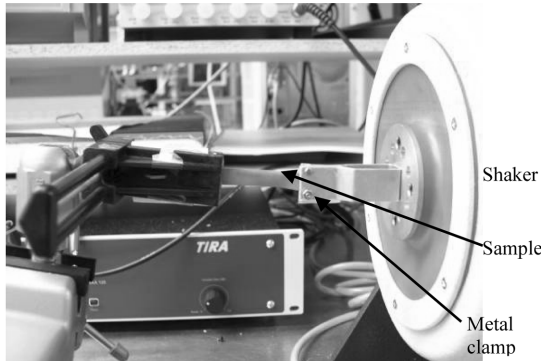


Fig. 8 Schematic of energy harvesting experimental set-up using shaker in tension mode



Fig. 9 Schematic of energy harvesting experimental set-up using shaker in shear mode

produce a sinusoidal mechanical vibration at a frequency (10Hz) different from the resonance frequency of IPMC samples. One end of the sample is clamped while the other end is pinned to the shaker shaft to have a better control on the sample motion. The displacement of the shaker is adjusted to 0.1786", 0.1985" and 0.5" in order to provide constant angular displacement of 11.4° for samples L1, L2 and L3 respectively. Under dynamic excitation, IPMC produces a sinusoidal waveform. In order to store the sensor output on a battery, the signal is converted to DC using a full bridge rectifier circuit. The rectified signal is used for charging a capacitor followed by a battery placed in parallel to the capacitor (Sodano, *et al.* 2004). The current stored on the 30 mAh rechargeable NiMH battery is connected to an IOTech Personal Daq 56 data acquisition system.

3.2. Extension mode

Experimental set-up for the extension mode is shown in Fig. 8. The metal clamp is manufactured to hold one end of the sample. Arrangements are made to electrically insulate the sample from the clamp. The shaker is excited using a biased sinusoidal signal from function generator (Wavetech, model 22) in order to produce shaker displacement in one direction. Three different frequencies are utilized for the sample excitation. Tests are performed using gold and platinum based IPMC samples. Other end of the sample is clamped to the electrode clasper for measuring the output signal produced on sample extension. The signal produced is transmitted to the energy harvesting circuit and stored using data acquisition box.

3.3. Shear mode

Experimental set-up for shear mode is shown in Fig. 9. The samples of 63 mm × 8.6 mm × 0.2 mm with Platinum and Gold electrodes are used for the experiment. The sample is treated with ionic liquid for enabling air operation without loss in its performance. Shaker assembly is programmed to vibrate at 10Hz frequency with displacement of its shaft at 0.5 inches. Both ends of the sample are clamped to respective clasper. Top clam is used for the extraction of the signal. The output of the sample is stored on a NiMH battery connected to the energy harvesting circuit.

Table 3 Sample dimensions

Sample Name	Free length [mm]	Width [mm]	Thickness [mm]
L1	22.5	8.60	0.20
L2	25.0	8.60	0.20
L3	63.0	8.60	0.20
W1	61.0	4.40	0.20
W2	61.0	8.60	0.20
W3	61.0	2.70	0.20
T1	61.0	4.40	0.17
T2	61.0	4.40	0.20

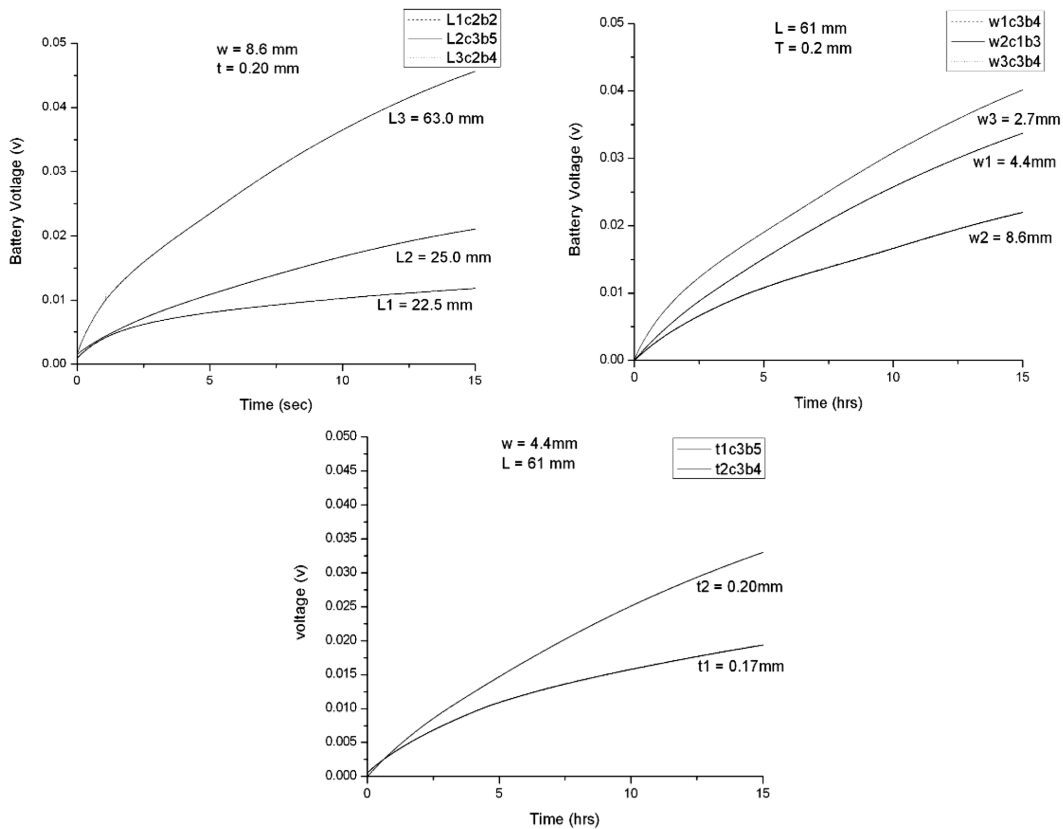


Fig. 10 Battery voltage produced by Platinum IPMC in bending mode using samples of different dimensions

4. Result and discussion

4.1. Battery charging

4.1.1. Bending mode

Experiments are conducted with three different lengths, three different width and two different

thicknesses of ionic liquid treated IPMC. Table 3 summarizes the dimension of samples used for experiments. The result of vibrating samples of different dimensions is shown in Fig. 10.

It can be concluded that a longer, less wide and thicker IPMC sample charges the battery more. This may be because the capacitance ' C ' is related to area and distance between the plates as:

$$C = \frac{\epsilon w l}{t} \quad (21)$$

where, C is the capacitance, w , l and t is the width, length and thickness of the sample respectively. So for a longer sample the charge stored on the capacitor is more than shorter sample:

$$Q = CV \quad (22)$$

where, Q is the charge on the capacitor electrodes and V is the voltage difference between the electrodes. A thicker IPMC sample shows better battery charging because a thicker sample will have more free ions associated with it although the capacitance from the electrode is assumed to be the same. Besides, it takes longer time for the ions to reach from one electrode to another on bending causing longer flow of current before they reach equilibrium. For a wider sample it appears that surface losses due to increase in surface resistivity are more. Therefore, less wide sample shows better battery charging.

Further experiments are conducted in order to compare the battery charging by Platinum and Gold based samples. Both the samples are made using the electroless plating method. Despite close control, it is difficult to match the thickness of the electrodes accurately, hence some difference in the result may be observed between the samples. As shown in Fig. 11, Platinum IPMC shows better charging than gold IPMC despite gold having lower surface resistivity. It is our belief that this is because Platinum IPMC produces better output voltage than Gold IPMC. The charging of the capacitor and subsequently the rate of battery charging is higher at the initial time. After 5 hrs the rate charging of both capacitor and the battery reduces.

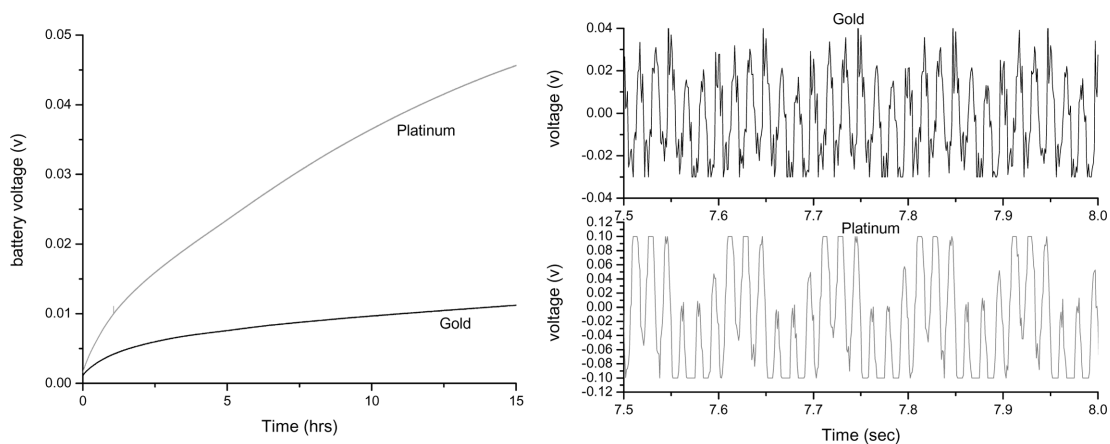


Fig. 11 Battery voltage produced by Pt and Gold IPMC and corresponding output voltage

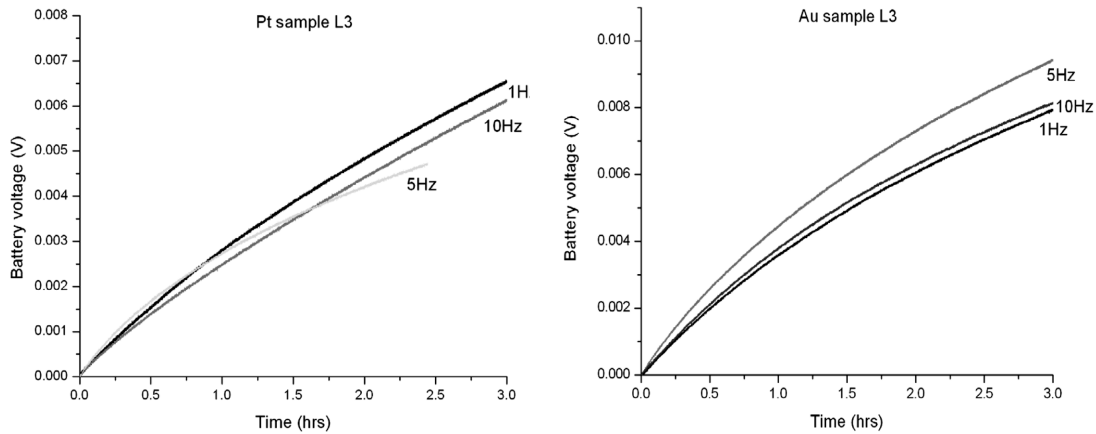


Fig. 12 Battery voltage produced by Platinum (left) and Gold IPMC in tension mode

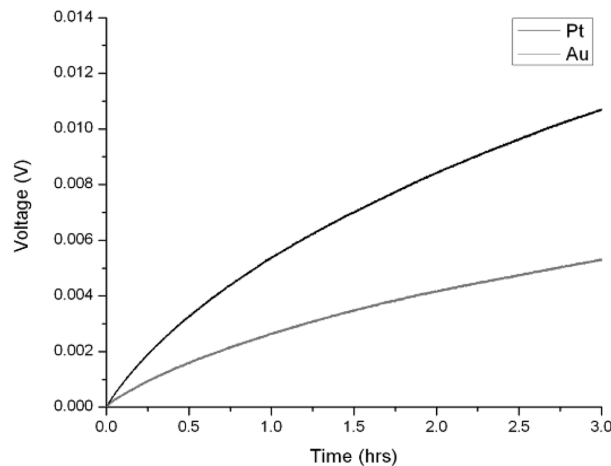


Fig. 13 Battery voltage for Platinum and Gold IPMC sample in shear mode

4.1.2. Tension mode

The voltage stored on the NiMH battery using Platinum and Gold IPMC (dimension $63 \times 8.6 \times 0.20 \text{ mm}^3$) is shown in Fig. 12. The graph depicts that battery charging is independent of the frequency of mechanical vibration. These frequencies are randomly picked, to demonstrate suitability for practical applications.

4.1.3. Shear mode

Both gold and platinum electrode IPMCs are excited in shear mode using shaker assembly at 10Hz frequency. This case is similar to bending mode except that the sample is bent side ways. Rectified IPMC signal from the sample is stored on a NiMH battery using data acquisition. Fig. 13 shows recorded battery voltage for 3 hrs. It can be concluded from the graph that Platinum shows better charging than Gold IPMC for a sample size of $63 \text{ mm} \times 8.6 \text{ mm} \times 0.2 \text{ mm}$.

4.1.4. Platinum versus gold IPMC

Battery charging as well as instantaneous power dissipation for platinum and gold IPMC was

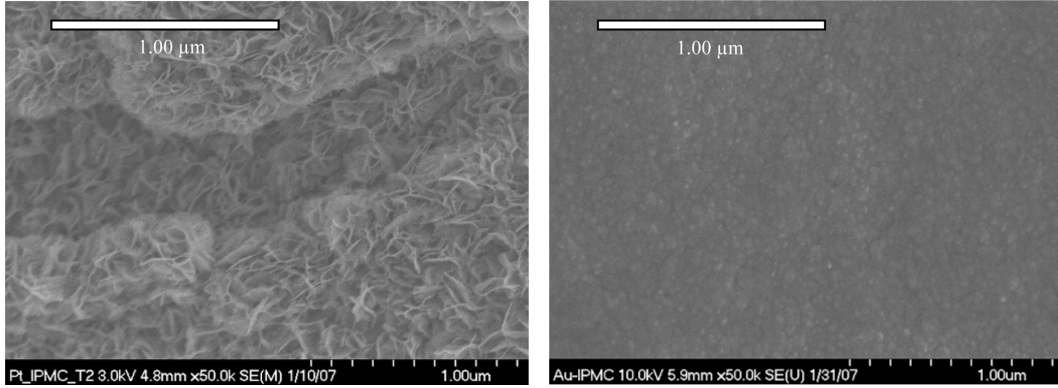


Fig. 14 SEM image of Pt (left) and Gold (right) IPMC

observed to be different in different modes. This variation may be accounted for by considering the morphology of the two types of IPMC shown in Fig. 14. As observed from the SEM image, gold IPMC surface is smoother and denser than the platinum IPMC. Besides, Platinum-IPMC surface displays rod structure. Thus in extension mode Gold-IPMC shows better charging due to more reduction in surface resistivity on stretching. On the other hand, Platinum-IPMC shows better charging in bending and side bending (shear) mode due to better distribution of platinum particles inside Nafion membrane.

4.1.5. Bending mode simulation results

A comparison of the analytically calculated force and measure force is shown in Fig. 15(a), using SIMULINK model, for the sample L3. It can be seen from the graphs that the signal generated using the simplified model produced reasonable result. From Eq. (20) we can find a sensor output equation as:

$$\frac{v}{\dot{u}} = Zm_1 = \frac{1}{s} \frac{Ywt^3}{4L_{free}^3} \tag{23}$$

This equation related the voltage produced by the sample when a measure displacement is applied to

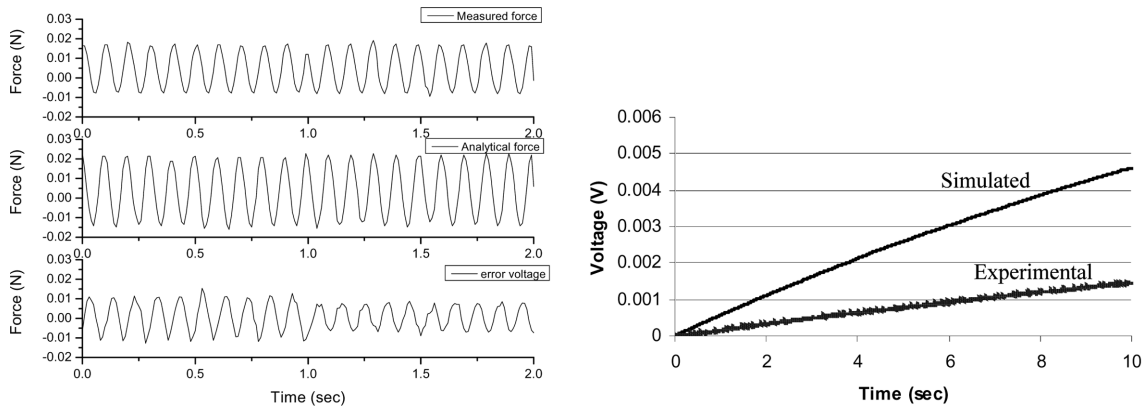


Fig. 15 Comparison of (a) analytical force derived using sensor model with measured force, (b) capacitor voltage using sensor model with the experimental result

the tip sample. This produced voltage signal is then used to charge a capacitor. The result of capacitor charging using SIMULINK is also shown in Fig. 15(b). For the convenience of representation of the result the simulation time of only a few seconds is illustrated in the figure. It appears that the modeling overestimates the charging capability of the IPMCs. Further investigation is needed to look into the incorporation of the mechanical damping and surface resistivity changes under applied deformations.

4.2. Instantaneous power dissipation at optimal load condition

It is important to determine power generated by IPMCs to identify its feasibility for real world applications. Instantaneous power is calculated by measuring voltage drop ‘ V ’ across load resistance, ‘ R .’

$$P = V^2/R \tag{24}$$

Experiments are conducted to determine the optimal resistive load for both Platinum and Gold based IPMC samples in bending, extension and shear mode as summarized in Fig. 16. Optimal resistive load for maximum power dissipation is experimentally evaluated to be 38 K for both Platinum and Gold IPMC for bending mode. It is clearly evident from the graph that in bending mode Platinum sample produces more power as compared to Gold sample. The resistive load of 38 K for Platinum and 1 MΩ

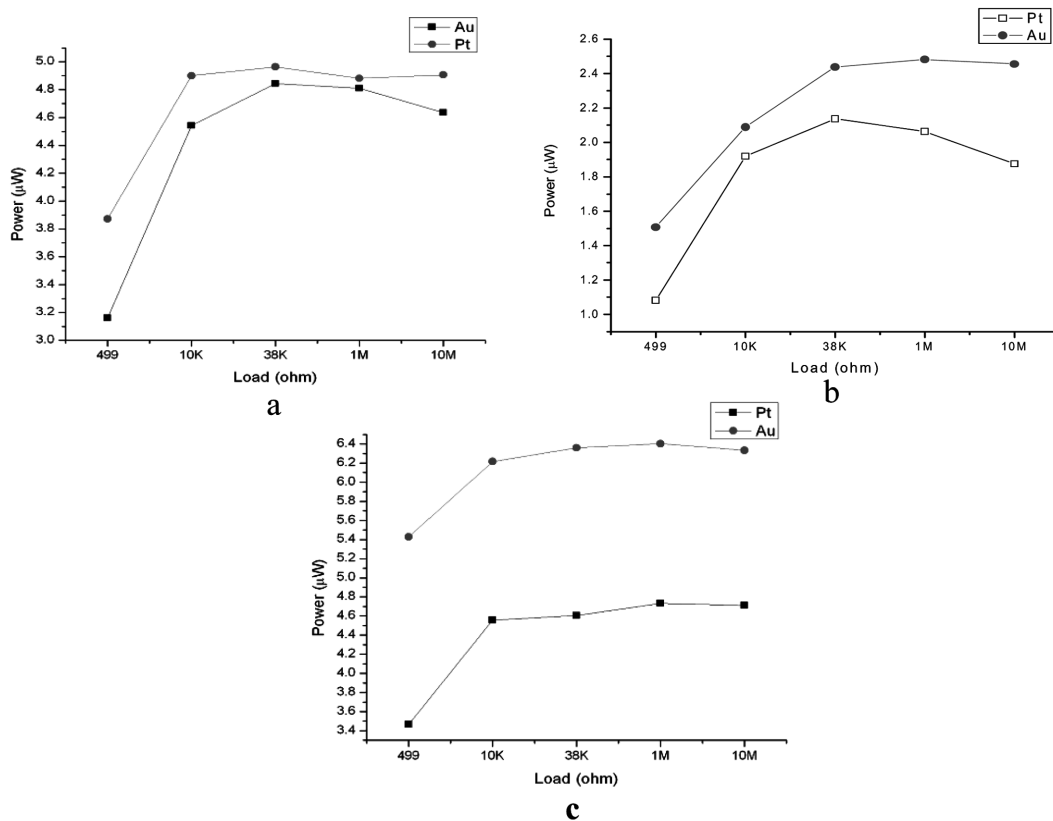


Fig. 16 Power dissipation as a function of resistive load in Platinum and Gold IPMC sample in (a) bending, (b) extension and (c) shear mode

Gold IPMC sample is optimal in extension mode. Maximum power dissipated at the optimal load is $2.1 \mu\text{W}$ for Platinum IPMC sample and $2.4 \mu\text{W}$ for Gold IPMC sample of the same dimension. Power dissipated by Gold IPMC is higher than Platinum IPMC sample. Similarly, instantaneous power dissipation from Gold IPMC sample is more than its Platinum counterpart in shear mode. Optimum resistive loading condition for both the sample is found to be $1 \text{ M}\Omega$.

5. Conclusions

The purpose of paper was to demonstrate the capability of IPMC as energy harvester. Effect of electrode type and sample dimensions was studied using a shaker system. Two different electrodes (gold and platinum) were employed for further understanding the effectiveness of different mechanical deformations: bending, tension and shear, for energy harvesting. Platinum IPMC illustrated better charging in bending and shear mode while Gold IPMC showed better battery charging in extension mode. These basic deformations may be combined for the development of 3D energy harvesting using IPMC. A simplistic electromechanical model was developed to provide an insight into the sensing mechanism of IPMC. The model does not take into account the effect of frequency on the material property. The model was thought to be useful for the feasibility study stated in the paper. Optimal resistive loading conditions are determined for Gold and Platinum IPMC samples using different resistances. Thus IPMC based energy harvester may be successfully employed as the continuous source of energy with no maintenance and virtually infinite lifetime. These harvesters may be used for air based as well as water based applications. Further work is required to develop physics based model to describe charge generation phenomenon under mechanical deformations and electrode surface morphology. It is also required to study the efficiency of IPMC based energy harvesters for better comparison with the existing technologies. Future work will stress on effect of cations on energy harvesting. Experiments will also be performed using different electrodes like palladium and platinum-palladium. A combination of electroplating with electroless plating will also be used for developing IPMCs.

Acknowledgement

The authors thank the partial financial support from the U.S. National Science Foundation.

References

- Akle, B. J., Bennett, M. D. and Leo, D. (2006), "High strain ionomeric-ionic liquid electroactive actuators, This paper came out: so more infor is provided herein", *Sensors and Actuators: A*, **126**(1), 26 January, p. 173-181.
- Bar-Cohen, Y., Bao, X., Sherrit, S. and Lih, S.-S. (2002), "Characterization of the electromechanical properties of ionomeric polymer metal composite", *Proceedings of the SPIE Smart Structures and Materials Symposium*, EAPAD Conference, San Diego, CA.
- Bar-Cohen, Y. (2002), "Electro-active polymers: Current capabilities and challenges", *Proceedings of SPIE the international society for optical engineering*, **4695**, 1-7.
- Bonomo, C., Negro, C. D., Fortuna, L. and Graziani, S. (2003), "Characterization of IPMC strip sensorial properties: preliminary results", *Proceedings of International Symposium on Circuits and Systems*, IV-816-IV-819.

- Dogruer D. (2006), "The development of a hydrodynamic model for the segmented ionic polymer metal composite (IPMC) for underwater applications and the potential use of IPMCs for energy harvesting", M.S. Thesis, University of Nevada, Reno, NV, U.S.A.
- Kim, K. J., Paquette, J., Leo, D. and Farinholt, K. M. (2006), "Ionic polymer metal composite for sensory applications", *Encyclopedia of Sensors*, 1-20.
- Konyo, M., Konishi, Y., Tadokoro, S. and Kishima, T. (2004), "Development of velocity sensor using ionic polymer metal composites", *Proceedings of the SPIE*, **5385**, 394.
- Kothera, C. S. (2002), "Micro-manipulation and bandwidth characterization of ionic polymer actuators", *Masters Thesis*, Virginia, Blacksburg.
- Lee, S., Park, H. C. and Kim, K. J. (2005), "Equivalent modeling of ionic polymer metal composite actuators based on beam theory", *Smart Mater. Struct.*, **14**, 1363-1368.
- Martin, B. R. (2005), "Energy harvesting applications of ionic polymer", Master Thesis, Virginia, Blacksburg.
- Newbury, K. (2002), "Characterization, modeling, and control of ionic polymer transducers", PhD Thesis, Virginia Tech, Blacksburg, VA.
- Newbury, K. and Leo, D. J. (2002), "Electromechanical modeling and characterization of ionic polymer benders", *J. Intell. Mater. Syst. Struct.*, **13**, 51-60.
- Paradiso, J. A. and Starner, T. (2005), "Energy scavenging for mobile and wireless electronics", *IEEE Pervasive Comput.*, **4**(1), 18-27.
- Shahinpoor, M. and Kim, K. J. (2005), "Ionic polymer metal composites IV: industrial and mechanical application", *Smart Mater. Struct.*, **14**, 197-214.
- Sodano, H. A., Inman, D. J. and Park, G. (2004), "A review of power harvesting from vibration using piezoelectric materials", *The Shock Vib. Digest*, **36** (3), 197-205.